Defining the Upper Nisyros Pumice (57.1 ± 1.5 ka) as new tephra isochrone for linking early MIS-3 palaeoenvironmental records in the Aegean-Black Sea gateway: New evidence from the Sea of Marmara

Sabine Wulf, M Namik Çağatay, Oona Appelt, K Kadir Eriş, Pierre Henry

Defining the Upper Nisyros Pumice (57.1 ± 1.5 ka) as new tephra isochrone for linking early MIS-3 palaeoenvironmental records in the Aegean-Black Sea region: new evidence from the Sea of Marmara

Sabine Wulf[1*], M. Namık Çağatay[2], Oona Appelt[3], K. Kadir Eriş[2], and Pierre Henry[4]

[1] School of the Environment, Geography and Geosciences, University of Portsmouth, Lion Terrace, Portsmouth, PO1 3HE, United Kingdom

[2] İstanbul Technical University, EMCOL Research Centre and Department of Geological Engineering, Ayazağa, 34469, İstanbul, Turkey

[3] Helmholtz Centre Potsdam, GFZ German Research Centre of Geosciences, Section 3.6, Telegrafenberg, 14473 Potsdam, Germany

[4] CEREGE (UMR7330), Aix-Marseille Université, CNRS-IRD, 13330, Marseille 7, France

*Corresponding author: sabine.wulf@port.ac.uk (S. Wulf)

Keywords: Cryptotephra, Upper Nisyros Pumice, Sea of Marmara, Eastern Mediterranean

Abstract

The rhyolitic Upper Nisyros Pumice (UNP) from the Kos-Yali-Nisyros volcanic system has been detected as a cryptotephra layer in lacustrine sediments from the Sea of Marmara (SoM). A new independent age of the UNP eruption at 57.1 ± 1.5 cal ka BP has been interpolated using a combination of radiocarbon dating, tephrochronology and wiggle-matching of the SoM proxy record (Ca-curves) with Greenland oxygen isotope data, therewith confirming recently published radioisotopic dates of UNP land deposits. The UNP tephra in the SoM was identified by comparisons of the SoM tephra glass chemical dataset with published data of other marine tephra records from the Aegean Sea and the Megali Limni lacustrine sediment sequence (Lesvos Island). The stratigraphic position of the UNP tephra in these records verified its deposition in the SoM at the onset of MIS-3 and specifically at the termination of Greenland Interstadial GI-16. The new findings define the UNP tephra as a valuable time marker for the synchronisation of palaeoenvironmental data for this time period and help spurring the

28 establishment of a robust tephrostratigraphical framework for the last ~70 kyr in the Aegean-
29 Black Sea region.

30 1. Introduction

31 Tephra layers in sedimentary records have been well established as tools for dating and
32 synchronizing palaeoclimate and -environmental data (e.g., Lowe, 2011), with numerous
33 examples derived from European records. Those include records from the Eastern
34 Mediterranean region which is characterised by intense and frequent explosive volcanic
35 activity (e.g., Italian and Aegean Arc volcanoes) and widespread tephra dispersal (e.g., Keller
36 et al., 1978; Narcisi and Vezzoli, 1999; Bourne et al., 2015; Satow et al., 2015; Giaccio et al.,
37 2012, 2019; Wulf et al., 2012, 2018, 2020; Vakhrameeva et al., 2018, 2019). To date,
38 numerous tephra markers from Italian volcanoes have been established as reliable isochrones
39 that provide precise and accurate absolute dates of the timing of their eruption (e.g., Giaccio
40 et al., 2012, 2017, 2019). However, dating of calc-alkaline tephras from Aegean Arc volcanoes
41 (e.g., Milos, Santorini, Kos, Nisyros, Yali) still lack absolute dating, mainly because advanced
42 radioisotopic dating techniques such as $^{40}K/^{40}Ar$ or $^{40}Ar/^{39}Ar$ are not suitable (e.g., Druitt et al.,
43 1999; Fabbro et al., 2013). One approach to overcome those dating problems is to interpolate
44 tephra deposition ages from sediment core chronologies of distal archives, as recently
45 demonstrated for Santorini tephra layers in Aegean Sea records (e.g., Satow et al., 2015,
46 2020; Wulf et al., 2020).

47 Compared to Santorini, the calc-alkaline Kos-Yali-Nisyros (KYN) magmatic system in the SE
48 part of the Aegean Sea still lacks a detailed tephrostratigraphy. Volcanic activity at the KYN
49 started approximately 3 Ma ago (Bachmann et al., 2010). One of the largest, caldera-forming
50 eruption occurred at 161.3 ± 1.1 ka resulting in the widespread dispersal of the Kos Plateau
51 Tuff (KPT; e.g., Smith et al., 1996; Hardiman, 1999; Allen, 2001). Subsequently, the volcanic
52 centres of Nisyros and Yali formed within the KPT caldera (Figs. 1a, c), which produced

several large explosive eruptions during the last 160 kyr (e.g., Pe-Piper and Moulton, 2008; Bachmann et al., 2012).

Nisyros activities in particular were characterised by alternating effusive and explosive cycles that erupted calc-alkaline basaltic-andesitic to rhyolitic lavas and pyroclastics (e.g., Di Paola, 1974; Limburg and Varekamp, 1991; Longchamp et al., 2011; Tomlinson et al., 2012a). Two major Plinian, caldera-forming events, the Lower (LNP) and Upper Nisyros Pumice (UNP) eruptions, formed massive tephra deposits on land and ash layers in distal terrestrial (Margari et al., 2007) and marine (e.g., Vinci, 1985; Hardiman, 1999; Aksu et al., 2008) settings. The timing of the LNP and UNP eruptions were controversially constrained to 110 - 28 ka (LNP; Rehren, 1988; Barberi et al., 1988; Hardiman, 1999; Aksu et al., 2008) and >50 - 35 ka (UNP; Vinci, 1985; Limburg and Varekamp, 1991; Margari et al., 2007; Karkanas et al., 2015), prohibiting for a long time the use of these tephras as reliable isochrones. However, recent advances in U-Th disequilibrium dating of zircon crystals have provided first absolute ages for the LNP and UNP eruptions at 63.1 ± 4.7 ka and 58.4 ± 2.7 ka respectively (Popa et al., 2020); those, however, still need verification by other independent dating techniques.

In this study, a comprehensive tephra glass chemical dataset and sediment accumulation rate age interpolation of a cryptotephra layer in sediments from the Sea of Marmara (SoM) is used to establish robust correlation and independent age control for the UNP eruption. The new dataset is used to re-evaluate previously published distal tephra findings in the Eastern Mediterranean region, with special focus on Nisyros tephra findings in the Megali Limni lacustrine sequence from Lesvos (Margari et al., 2007, 2009) and in Aegean Sea cores (Aksu et al., 2008; İşler et al., 2016). The results will help to develop a more robust tephrostratigraphical framework in the Aegean-Black Sea region for the last 70 kyr.

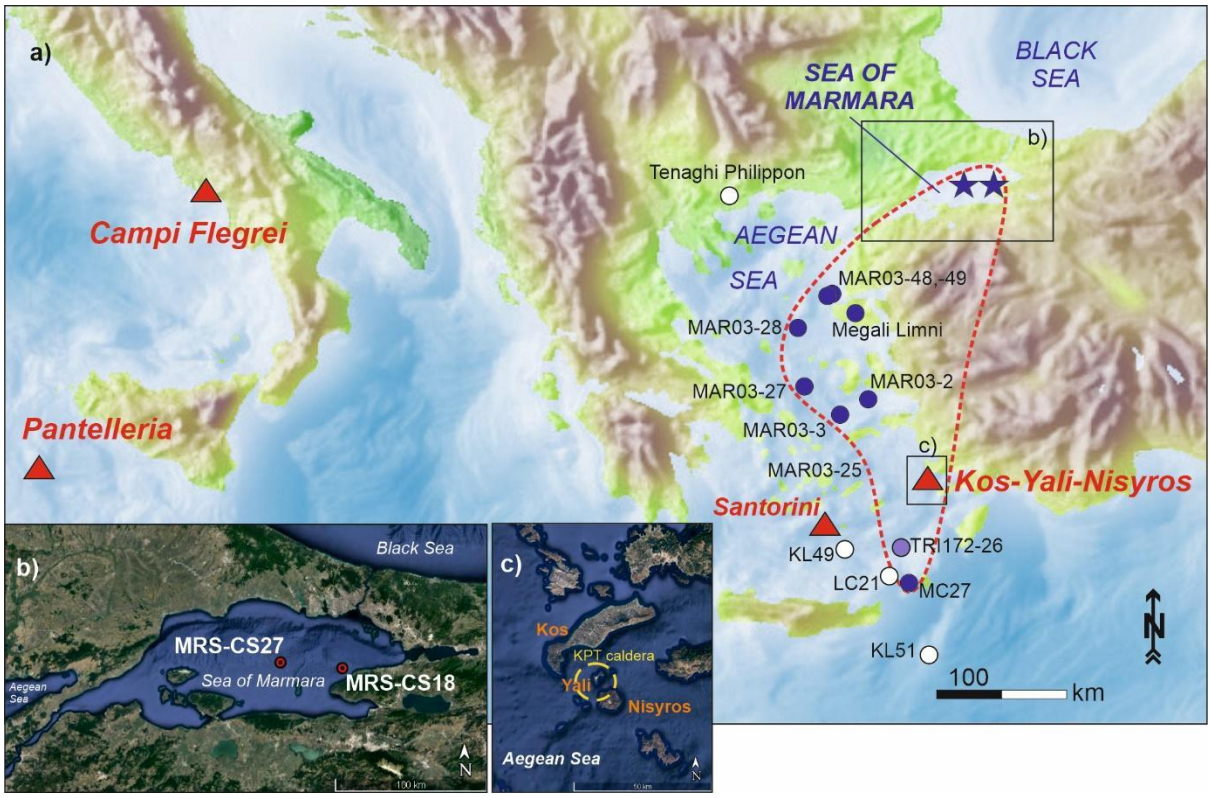

78 **Figure 1: a)** Topographic map of the Eastern Mediterranean depicting the coring locations of
79 MRS-CS18 and MRS-CS27 (blue stars) from the Sea of Marmara in relation to relevant
80 volcanic provinces (red triangles) and other marine and terrestrial archives (blue dots) with
81 Upper Nisyros Pumice occurrences. Tephra data are retrieved from Aksu et al. (2008) (MAR
82 sites), Vinci (1985) (site MC27), Hardiman (1999) (purple site TRI172-26 with undefined
83 Nisyros tephra occurrence), and Margari et al. (2007, 2009) (Megali Limni). White dots depict
84 sites that lack Nisyros tephra (Tenaghi Philippon, Wulf et al., 2018; LC21, Satow et al., 2015;
85 KL49, KL51, Wulf et al., 2020). The red dotted line indicates the proposed dispersal area of
86 the UNP (this study). **b)** GoogleEarth inlet map showing the detailed positions of cores MRS-
87 CS18 and MRS-C27 in the SoM (red dots). **c)** GoogleEarth inlet map of the Kos-Yali-Nisyros
88 volcanic complex with the inferred KPT caldera (dotted yellow line).

89 ## 2. Material and methods

90 Sediment cores used in this study derived from the central and eastern part of the SoM. The
91 SoM is a brackish water basin in the Eastern Mediterranean region that connects the saline
92 Aegean Sea and the Black Sea brackish water basin via the Dardanelles and Bosporus straits
93 (Figs. 1a, b). Cores MRS-CS18 and MRS-CS27 were retrieved in 2015 on board of the RV

Pourquoi pas? from 291 m below sea level (b.s.l.) and 313 m b.s.l. at the northeastern and western edges of the İmrali Basin in the SoM, respectively (Çağatay et al., 2019) (Fig. 1b). Sediments of both cores encompass alternating lacustrine and marine facies interrupted by a hiatus (Fig. 2) which indicates past major water level variations (Çağatay et al., 2019). Core MRS-CS18 is a 14.05 m long sequence that contains an 8-cm-thick brown tephra layer (CS18-MT2) at 2.03-2.11 mbsf and a 2-mm-thin ash layer (CS18-MT3) at 3.095 mbsf. Core MRS-CS27 comprises a 20.45 m long sediment sequences that shows three distinct tephra layers: the greyish CS27-MT1 (6.955-7.005 mbsf), the brownish CS27-MT2 (13.835-13.88 mbsf), and the mm-thin CS27-MT3 ash layer at 16.18 mbsf. Based on their similar stratigraphic positions and appearances in other SoM cores (Çağatay et al., 2015) the thick MT1 and MT2 tephra layers have been tentatively correlated to the Y-2/Cape Riva eruption of Santorini and the Y-5/Campanian Ignimbrite by Çağatay et al. (2019). The MT3 ash layer has been detected in cores MRS-CS18 and MRS-CS27 by studying sections of increased values in magnetic susceptibility and XRF-Calcium counts of sediments. Çağatay et al. (2019) roughly associated the MT-3 tephra with the marine X-1 tephra based on its chronostratigraphic position in both cores below the Campanian Ignimbrite (Çağatay et al., 2019). However, all these tentative tephra assignments still require verification by glass geochemical fingerprinting.

In this study, polished thin sections of tephra glass concentrate of the five tephra layers in cores MRS-CS18 (MT2, MT3) and MRS-CS27 (MT1, MT2, MT3) were used to determine the major element compositions of individual glass shards by electron probe microanalyses (Supplement A). Measurements were carried out at the GFZ Potsdam (Germany) using a JEOL-JXA8230 (WDS) probe with the following analytical setup: 15 kV accelerating voltage, 10 nA beam current and 8-10 µm beam size. Analytical count times were 20 seconds for the elements Fe, Mn, Ti, Mg, P, and Cl, and 10 seconds for elements Si, Al, K, Ca, and Na measured first. The natural Lipari obsidian (Hunt and Hill, 1996; Kuehn et al., 2011) and artificial glass standards from the Max Planck Institute (MPI-glasses: ATHO-G, StHs6/80 and GOR-132; Jochum et al., 2006) were used for data quality insurance (Supplement A).

Correlation of MT tephras used bivariate elemental plots of MT glass data and published glass datasets (Fig. 3).

MT3 tephra ages in SoM cores have been constrained by slightly revising the original age-depth models of cores MRS-CS18 and MRS-CS27 (Çağatay et al., 2019), which are based on a combination of wiggle-matching of the XRF-Ca-curves of both cores with interstadials of the NGRIP oxygen isotope curve (Andersen et al., 2006; Svensson et al., 2008; Wolff et al., 2010), radiocarbon dates on fossil shell samples, and tephrochronology (Fig. 2, Supplement A, Supplement Fig. B1). The revised sediment chronologies used the newest INTCAL20 version by Reimer et al. (2020) for radiocarbon age calibration as well as up-to-date published tephra ages (Supplement Table B1). Tephra ages were calculated as average values from the 2σ age ranges that were obtained by Bayesian modelling using the OxCal version 4.4.3 (Bronk Ramsey, 2021) (Supplement A). The revision of the original chronology of the Megali Limni lacustrine sequence ML01 (Margari et al., 2007, 2009) to estimate ages of potential Nisyros tephra equivalents used the same approach (see details in Supplement Fig. B2, Supplement C).

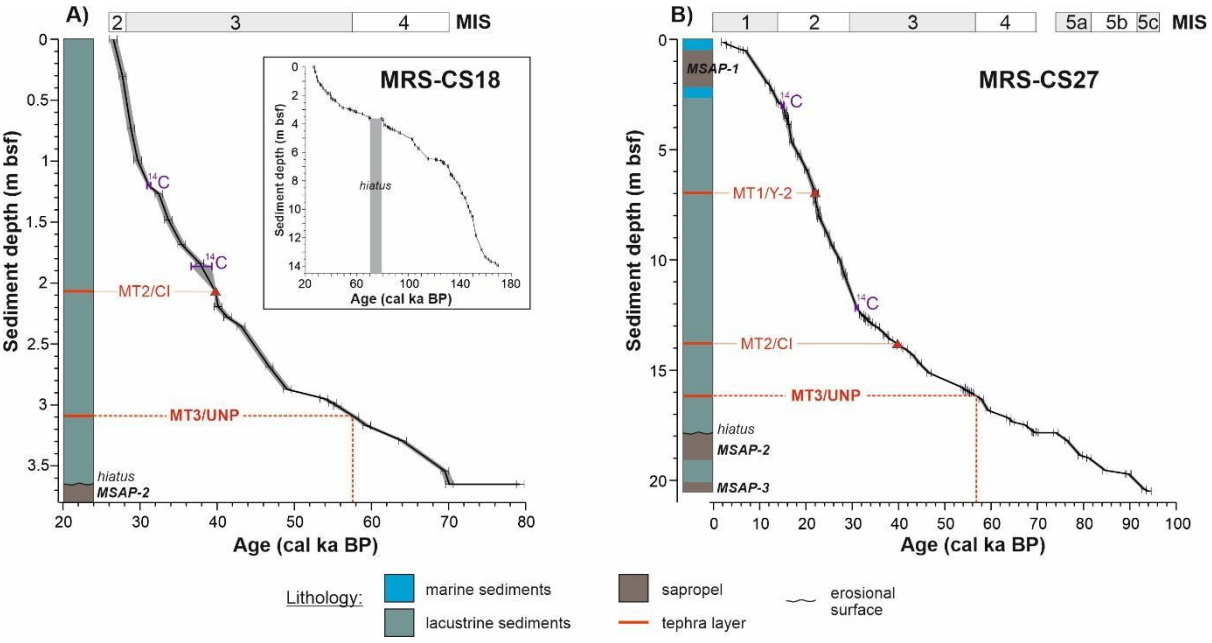

Figure 2: Lithologies and age-depth models of Sea of Marmara cores MRS-CS18 **(a)** and MRS-CS27 **(b)** for the interval of the last 70 kyr. The inlet graph (a) depicts the complete chronology of core MRS-CS18 as described in Çağatay et al. (2019). Core chronologies are based on a combination of radiocarbon dates (purple bars), imported tephra ages (red triangles) and wiggle-matching with the NGRIP oxygen isotope record (black bars). The MT3/UNP tephra ages (red dotted lines) derive from Bayesian modelling (Supplement A). MSAP represents typical sapropel layers in the Sea of Marmara, after marine re-connections during the interglacial periods.

3. Results

Tephras MT1 and MT2 in both SoM cores have rhyolitic and phono-trachytic major element glass compositions that confirm the proposed correlation by Çağatay et al. (2019) to the Y-2/Cape Riva and Y-5/Campanian Ignimbrite tephras, respectively (Fig. 3a, Supplement A). Therefore, the published eruption ages for the Y-2 (22.02 ± 0.64 cal ka BP; Bronk Ramsey et al., 2015) and Y-5 tephras (39.85 ± 0.14 $^{40}Ar/^{39}Ar$ ka, 39.78 ± 0.14 cal a BP; Giaccio et al., 2017) were implemented as independent time markers for the construction of the revised age-depth models (Fig. 2).

The glass composition of the MT3 cryptotephra layer is high-silica rhyolitic with concentration ranges in SiO_2 of 76.5-78.4 wt%, Al_2O_3 of 11.9-12.6 wt%, FeO of 0.6-1.6 wt%, CaO of 0.7-1.2 wt%, K_2O of 3.6-4.9 wt%, and total alkalis (Na_2O+K_2O) of 7.1-8.3 wt% (normalised data) (Supplement A). This major element glass chemistry is typical for tephras from the eastern Aegean Arc and particularly from the Kos-Yali-Nisyros volcanic system. The MT3 glass chemistry clearly matches the glass composition of the proximal deposits of the Upper Nisyros Pumice (Tomlinson et al., 2012a), which can be well discriminated from the Lower Nisyros Pumices (LNP) by slightly higher mean values in SiO_2 (77.2 *vs.* 76.1 wt%) and lower concentrations in Al_2O_3 (12.3 *vs.* 12.9 wt%), FeO (1.3 *vs.* 1.5 wt%) and Na_2O (3.3 *vs.* 3.7 wt%) (Figs. 3b-c).

The timing of the MT3 tephra deposition in the SoM has been interpolated by the revised age-depth models of the MRS-CS18 and MRS-CS27 cores at 57,440 ± 1570 cal a BP and 56,710 ± 1420 cal a BP, respectively (Fig. 2). The mean age yields at 57,080 ± 1,500 cal a BP, which agrees well within its 2σ uncertainty with the U-Th disequilibrium (zircon) age of the proximal Upper Nisyros Pumice deposits at 58.4 ± 2.7 ka BP obtained by Popa et al. (2020). Furthermore, the chronostratigraphic position of the MT3 tephra as inferred from wiggle-matching of the SoM Ca-curves with Greenland isotope data suggests a deposition in both cores at the termination of Greenland Interstadial GI-16 (Fig. 4b-c).

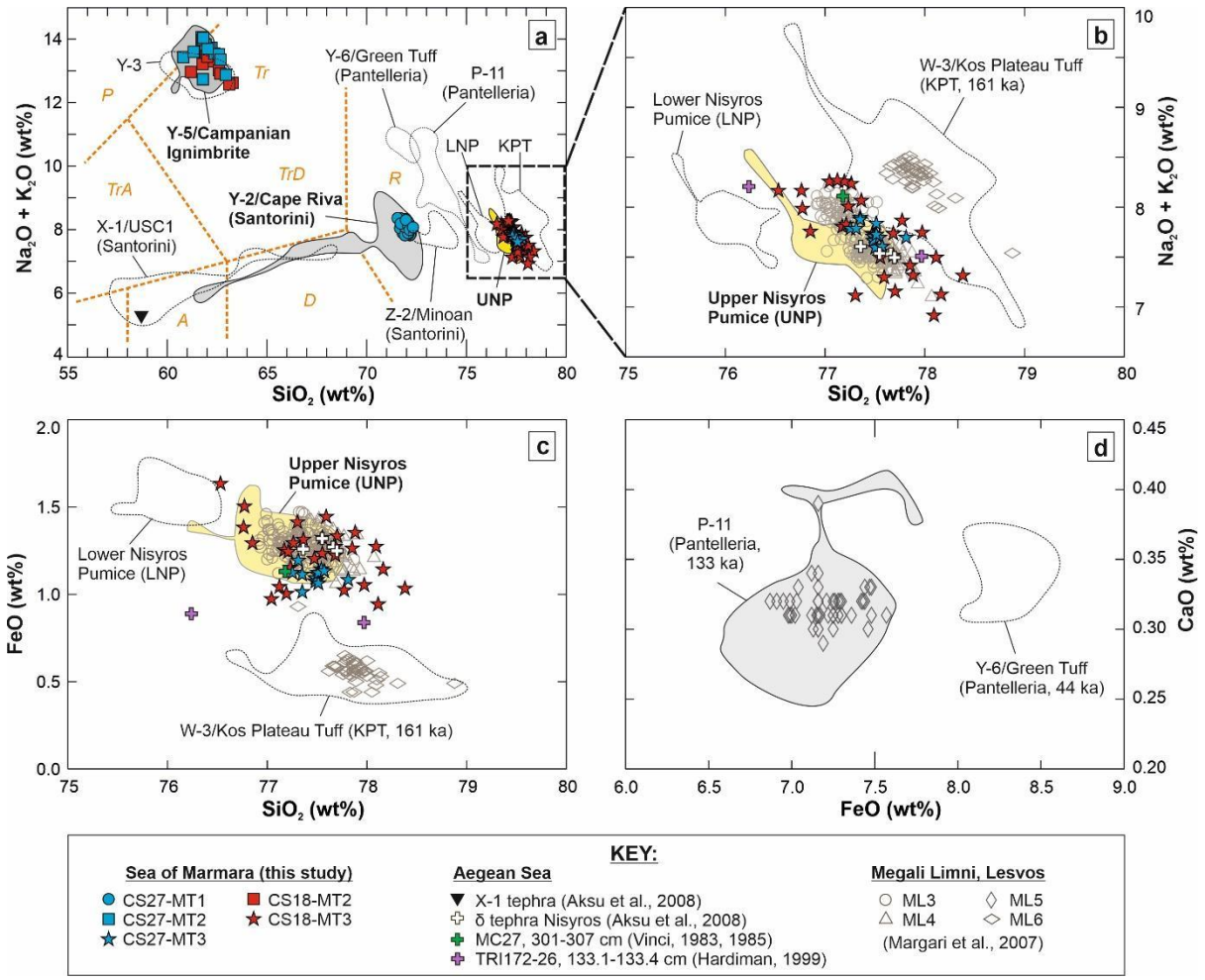

Figure 3: (a-d) Bivariate elemental plots of glass compositions of MT tephras of the Sea of Marmara cores (this study), compared with published tephra datasets (envelopes) and potential distal correlatives from the Aegean Sea (Aksu et al., 2008; Vinci, 1983, 1985;

Hardiman, 1999) and Megali Limni, Lesvos Island, Greece (Margari et al., 2007). Tephra glass chemical datasets are retrieved from: *Z-2/Minoan and Y-2/Cape Riva*: Kwiecien et al. (2008), Tomlinson et al. (2015), Wulf et al. (2018, 2020); *Y-3*: Albert et al. (2015), Wulf et al. (2018, 2020); *Y-5/Campanian Ignimbrite*: Tomlinson et al. (2012b), Wulf et al. (2018); *Y-6/Green Tuff*: Tomlinson et al. (2015); *X-1/Upper Scoriae 1*: Wulf et al. (2020); *P-11*: Satow et al. (2015), Vogel et al. (2010), Leicher et al. (2016); *Lower and Upper Nisyros Pumice (LNP, UNP)*: Tomlinson et al. (2012a); *W-3/Kos Plateau Tuff*: Satow et al. (2015), Wegwerth et al. (2019), Wulf et al. (2020).

4. Discussion

The comparison with distal tephra datasets shows that the MT3 tephra from the SoM correlates with the rhyolitic tephra δ identified in several Aegean Sea cores (Aksu et al., 2008; İşler, 2012; İşler et al., 2016), with a Nisyros tephra in southern Aegean Sea core MC27 (301-307 cm depth; Vinci, 1983, 1985), and with the ML3 and ML4 layers in the lacustrine core ML01 from Megali Limni, Lesvos Island, Greece (Margari et al., 2007, 2009) (Figs. 3b-c). There is only a vague compositional overlap with a proposed Lower Nisyros Pumice tephra in Adriatic Sea core TRI172-26 (133.1-133.4 cm depth; Hardiman, 1999) (Figs. 3b-c), and the MT3 glass chemistry is clearly distinct from the andesitic composition of the marine X-1 tephra in the Aegean Sea (Fig. 3a).

Notably, the previous lack of glass chemical data of Nisyros tephra land deposits has for long prevented reliable tephra correlations for the above-mentioned sites, and, in the case of Megali Limni, partly confounded the core chronology and therewith the proxy data interpretations. Hence, the respective tephra datasets of these records have been re-evaluated within this study to allow for a direct comparison with SoM data (Fig. 4).

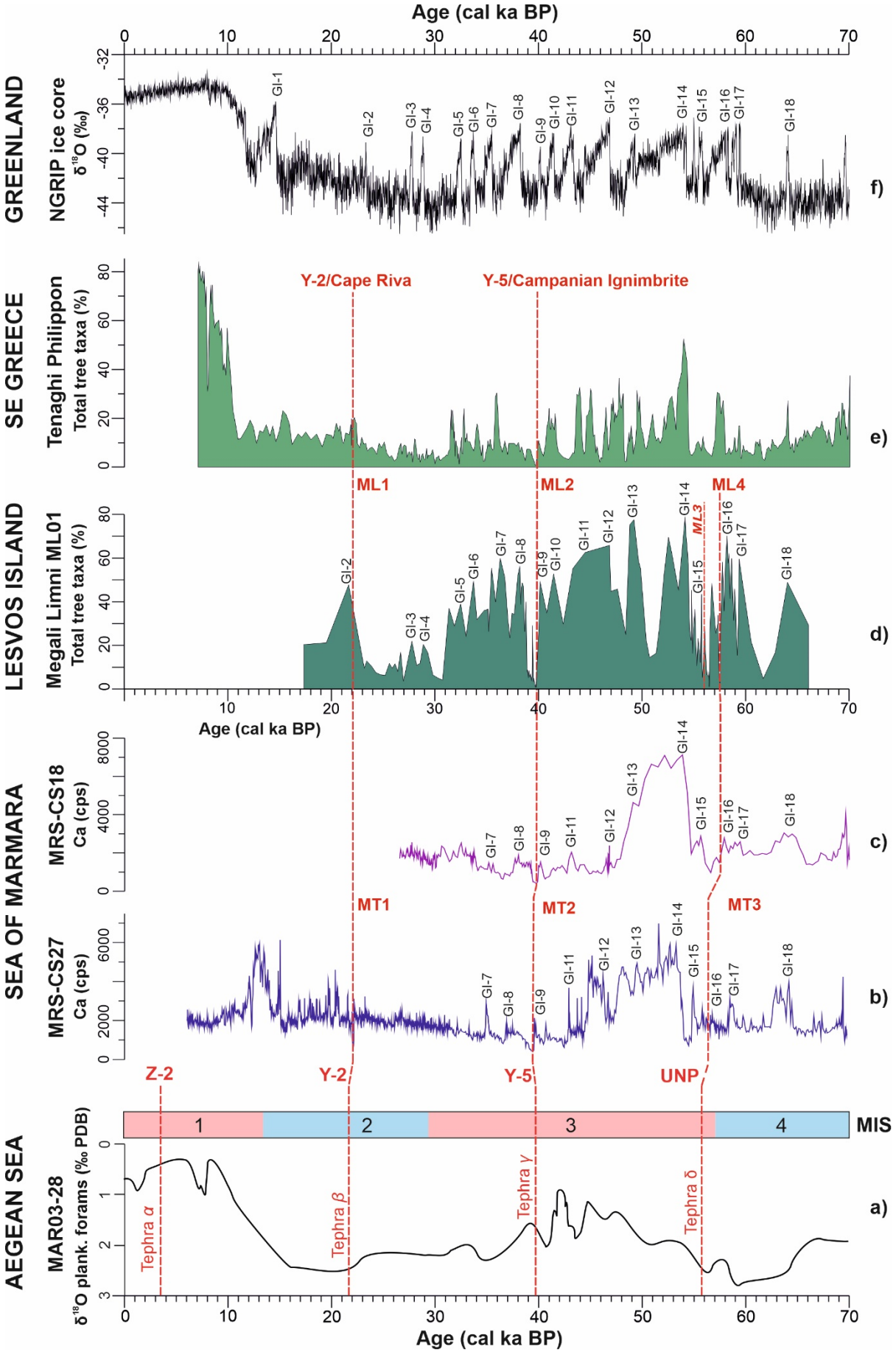
Age (cal ka BP)
GREENLAND
NGRIP ice core
δ18O (‰)
f)
SE GREECE
Tenaghi Philippon
Total tree taxa (%)
Y-2/Cape Riva
Y-5/Campanian Ignimbrite
e)
LESVOS ISLAND
Megali Limni ML01
Total tree taxa (%)
ML1
ML2
ML3
ML4
d)
SEA OF MARMARA
MRS-CS18
Ca (cps)
c)
MRS-CS27
Ca (cps)
MT1
MT2
MT3
b)
Z-2
Y-2
Y-5
UNP
MIS
AEGEAN SEA
MAR03-28
δ18O plank. forams (‰ PDB)
Tephra α
Tephra β
Tephra γ
Tephra δ
a)

Figure 4: Comparison of palaeoenvironmental records of the last 70 kyr from the Aegean-Black Sea region by using mutual tephra isochrons (red dotted lines). **a)** Oxygen isotope curve of planktonic foraminifera from Aegean Sea core MAR03-28 (İşler et al., 2016) with timescale of Marine Isotope Stages (MIS); XRF-Ca-records of core MRS-CS27 **(b)** and MRS-CS18 **(c)** from the Sea of Marmara (Çağatay et al., 2019; this study) with positions of wiggle-matched Greenland Interstadials (GI). **d)** Total tree pollen percentages in the Megali Limni sequence, Lesvos Island (Margari et al., 2009; Sánchez Goñi et al., 2017) on a revised timescale (this study; see also Supplement Fig. B2-B4 and Supplement C) and with positions of wiggle-matched GIs. **e)** Total tree pollen percentages of the Tenaghi Philippon peat sequence, Southeast Greece (Müller et al., 2011; Wulf et al., 2018); **f)** Oxygen Isotope record of Greenland ice core NGRIP (NGRIP members, 2004) with positions of Greenland Interstadials (GI).

4.1 Synchronisation with distal terrestrial tephra archives

The comparison of the MT3 tephra data with the tephrostratigraphic record of the lacustrine record of Megali Limni (Margari et al., 2007, 2009; Pyle and Margari, 2009) is quite complex and requires a thorough revision of the published dataset. Margari et al. (2007, 2009) identified six visible tephra layers, namely ML1 to ML6, in core ML01 for which the age of the oldest tephra ML6 has been interpolated to ~57.6 cal ka BP. The sequence contains two closely-spaced Nisyros tephra layers, ML3 and ML4 (Margari et al., 2007), with identical glass composition that is also comparable to that of the UNP proximal deposits (Tomlinson et al., 2012a) and the SoM MT3 tephra (Fig. 3c-d). The deposition ages of the ML3 and ML4 tephra layers have been originally extrapolated to ~46.0 and ~46.8 cal ka BP (Margari et al., 2007; Pyle and Margari, 2009); those, however, are considerably younger than the UNP age constrained from the SoM sequences in this study.

The original age-depth model of the Megali Limni sequence is based on a combination of tephrochronology and radiocarbon dating (Margari et al., 2007). When reviewing the tephrochronological dataset, it is apparent that the youngest tephras ML1 and ML2, correlated by Margari et al. (2007) with the Y-2/Cape Riva and Y-5/Campanian Ignimbrite eruptions

respectively, are reliable time marker for the age-depth model. However, the two oldest tephras ML5 and ML6 have been miscorrelated, and their imported ages therefore significantly falsified the chronology. The younger ML5 tephra was previously correlated by Margari et al. (2007) to the Y-6/Green Tuff of Pantelleria (44.1 ± 0.6 ka; Scaillet et al., 2013). However, FeO values of ML5 tephra glasses are too low to justify an assignment to the Y-6 tephra but rather suggest a correlation with the older Pantelleria P-11 tephra (133 ka; Satow et al., 2015) (Fig. 3d). A correlation with the P-11 tephra has been also postulated by Vogel et al. (2010) and is strongly supported by the widespread dispersal of this tephra in the Balkan (e.g., Vogel et al., 2010; Karkanas et al., 2015; Leicher et al., 2016) and southern Aegean Sea (Satow et al., 2015) regions. The ML6 tephra, on the other hand, has been previously assigned to an unknown Aegean Arc tephra (Margari et al., 2007) despite its glass composition showing an unambiguous chemical match with the marine W-3 and the Kos Plateau Tuff (KPT; 161.3 ± 1.1 ka, Smith et al., 1996) (Fig. 3b-c). The stratigraphic position below the 133 ka-Pantelleria tephra and the fact that the KPT is present in marine records from the Aegean-Black Sea region (e.g., Satow et al., 2015; Wegwerth et al., 2019; Wulf et al., 2020) additionally support a correlation of ML6 to the W-3/KPT eruption.

When considering the tephra ages of the revised ML5/P-11 and ML6/KPT correlations and re-evaluating the Megali Limni pollen record of Margari et al. (2009) by wiggle-matching with the Tenaghi Philippon pollen and the Greenland oxygen isotope records (Fig. 4d-f), it is evident that the basal sediments of the Megali Limni core date back to the penultimate glacial instead of MIS 4 (Supplement Figs. B2-B4, Supplement C). The new ML01 chronology also provides revised modelled dates of the ML3 and ML4 tephras at 55,970 ± 2040 cal a BP and 57,490 ± 2030 cal a BP respectively (Fig. 4). The ML4 age at ~57.5 cal ka BP in particular agrees well and within 2σ uncertainties with the UNP/MT3 extrapolated age in the SoM sediments (~57.1 cal ka BP) and with the U-Th disequilibrium zircon date of proximal UNP deposits at ~58.4 ka by Popa et al. (2020). Furthermore, the ML4 tephra stratigraphic position in the Megali Limni pollen record confirms the occurrence of the UNP eruption at the

termination of Greenland Interstadial GI-16 (Fig. 4, Supplement Figs. B3-B4). The revised chronostratigraphic information in combination with the lack of proximal and marine distal evidence for more than one UNP eruption suggest that ML4 is most likely the primary tephra layer in the Megali Limni sequence and that the younger ML3 tephra layer might have been derived from reworking processes which, however, needs to be further investigated.

4.2 Links with marine tephra archives and UNP dispersal

The majority of Nisyros tephra findings derives from the marine realm. For example, Aksu et al. (2008) identified the thin 'tephra δ' layer in several sediment cores collected from across the Aegean Sea and north of Nisyros volcano (MAR-sites in Fig. 1a). Tephra δ is stratigraphically positioned between the Campanian Ignimbrite tephra layer and sapropel S3 and has been dated by extrapolation of the marine oxygen isotope stratigraphy to originally 42-44 ka BP (Aksu et al., 2008). Higher-resolution $\delta^{18}O$ records published by İşler et al. (2016) have corrected this age to 53-58 ka BP, therewith placing tephra δ at the onset of MIS 3 (Fig. 4a). A previous correlation of tephra δ with the Lower Nisyros Pumice by Aksu et al. (2008) has been revised to the Upper Nisyros pumices by Tomlinson et al. (2012a), and the new SoM MT3 dataset corroborates this assignment (Figs. 3b-c). Therewith, the UNP tephra, together with the Campanian Ignimbrite and the Santorini Y-2, presents an additional valuable isochrone for the glacial period that allows for detailed palaeoceanographic reconstructions of the Aegean-Black Sea region (Fig. 4).

Other UNP tephra findings in the Aegean Sea include a 6-cm-thick layer in core MC27, located ~120 km south of Nisyros (Vinci, 1983, 1985). The chronostratigraphic position of the MC27 tephra is only poorly constrained, hence impeding a direct comparison with the SoM and other Aegean Sea data. Nevertheless, the MC27 tephra plays an important role for reconstruction of the UNP tephra dispersal in the Aegean Sea region since its occurrence indicates an additional southerly dispersion alongside the predominant northerly dispersal

pattern as evidenced from the MAR Aegean Sea, Megali Limni, and SoM cores. However, MC27 is to date the only distal core south of Nisyros containing the UNP tephra, while other nearby high-resolution tephra archives, i.e. cores LC21 (Satow et al., 2015), KL49 and KL51 (Wulf et al., 2020) lack this tephra (Fig. 1a). Therefore, further investigations are required to demonstrate the primary character of the MC27 tephra prior to interpret this complex dispersal pattern.

5. Conclusions

The new findings of the Upper Nisyros Pumice as MT3 tephra in the Sea of Marmara in combination with high-resolution proxy datasets provided a new modelled age of the UNP eruption at 57.1 ± 1.5 cal ka BP. This tephra age confirms the radioisotopic date of the UNP by Popa et al. (2020) and agrees well with the revised modelled age of the UNP distal tephra equivalent ML4 in the Megali Limni terrestrial record. The stratigraphic position of the UNP in palaeoenvironmental records of the Aegean-Black Sea region suggests a deposition at the termination of Greenland Interstadial GI-16 (SoM, Megali Limni) and at the onset of MIS 3 (Aegean Sea cores).

The occurrence of the UNP tephra in the SoM represents to date the furthest finding in the north-eastern part of the Aegean-Black Sea region, suggesting likely a transport by strong prevailing southerly winds at the time of the eruption and implying the possibility to detect this tephra in even more distal positions than previously believed. It is therefore recommended that future palaeoenvironmental studies in this region implement detailed (crypto)tephra studies to take advantage of this new tephra isochrone.

Acknowledgements

We thank the scientific team of Marsite cruise and the captains and crews of RV Pourquoi pas? for the recovery of cores MRS-CS18 and MRS-CS2. The Marsite cruise was co-funded by the EC FP7 project MARSITE (grant number: 308417), the “Laboratoire d'Excellence” LabexMER (ANR-10-LABX-19) through the projects called Micro-GaMa and MISS Marmara, and by a grant from the French government under the program “Investissements d'Avenir”. We also thank Mehmet Ali Oral of Geological Enginering Department at ITU, for the preparation of polished thin sections for tephra EPM analysis.

References

Aksu, A.E., Jenner, G., Hiscott, R.N., Isler, E.B., 2008. Occurrence, stratigraphy and geochemistry of Late Quaternary tephra layers in the Aegean Sea and the Marmara Sea. Mar. Geol. 252, 174-192. https://doi.org/10.1016/j.margeo.2008.04.004

Albert, P.G., Hardiman, M., Keller, J., Tomlinson, E.L., Smith, V.C., Bourne, A.J., Wulf, S., Zanchetta, G., Sulpizio, R., Müller, U.C., Pross, J., Ottolini, L., Matthews, I.P., Blockley, S.P.E., Menzies, M.A., 2015. Revisiting the Y-3 tephrostratigraphic marker: a new diagnostic glass geochemistry, age estimate, and details on its climatostratigraphical context. Quat. Sci. Rev. 118, 105-121. https://doi.org/10.1016/j.quascirev.2014.04.002

Allen, S.R., 2001. Reconstruction of a major caldera-forming eruption from pyroclastic deposit characteristics: Kos Plateau Tuff, eastern Aegean Sea. J. Volcanol. Geoth. Res. 105, 141-162. https://doi.org/10.1016/S0377-0273(00)00222-5

Andersen, K.K., Svensson, A., Johnsen, S., S.O. Rasmussen, S.O., Bigler, M., Rothlisberger, R., Ruth, U., Siggaard-Andersen, M.L., Steffensen, J.P., Dahl-Jensen, D., Vinther, B.M., Clausen, H.B., 2006. The Greenland ice core chronology 2005, 15–42 ka. part 1: constructing the time scale. Quat. Sci. Rev. 25, 3246-3257. https://doi.org/10.1016/j.quascirev.2006.08.002

Bachmann, O., Schoene, B., Schnyder, C., Spikings, R., 2010. $^{40}Ar/^{39}Ar$ and U/Pb dating of young rhyolites in the Kos-Nisyros volcanic complex, Eastern Aegean Arc (Greece): age discordance due to excess ^{40}Ar in biotite. Geochem. Geophy. Geosy. 11, Q0AA08. https://doi.org/10.1029/2010GC003073

Bachmann, O., Deering, C.D., Ruprecht, J.S., Huber, C., Skopelitis, A., Schnyder, C., 2012. Evolution of silicic magmas in the Kos-Nisyros volcanic center, Greece: a petrological cycle associated with caldera collapse. Contrib. Mineral. Petr. 163, 151-166. https://doi.org/10.1007/s00410-011-0663-y

Barberi, F., Navarro, J.M., Rosi, M., Santacroce, R., Sbrana, A., 1988. Explosive interaction of magma with groundwater: insights from xenoliths and geothermal drillings. Rend. Soc. Ital. Mineral. Petrol. 43, 901–926. http://hdl.handle.net/11568/15177

Bourne, A.J., Albert, P.G., Matthews, I.P., Trincardi, F., Wulf, S., Asioli, A., Blockley, S.P.E., Keller, J., Lowe, J.J., 2015. Tephrochronology of core PRAD 1-2 from the Adriatic Sea: insights into Italian explosive volcanism for the period 200-80 ka. Quat. Sci. Rev. 116, 28-43. https://doi.org/10.1016/j.quascirev.2015.03.006

Bronk Ramsey, C., 2021. OxCal version 4.4.3. https://c14.arch.ox.ac.uk/oxcal.html.

Bronk Ramsey, C., Albert, P.G., Blockley, S.P.E., Hardiman, M., Housley, R.A., Lane, C.S., Lee, S., Matthews, I.P., Smith, V.C., Lowe, J.J., 2015. Improved age estimates for key Late Quaternary European tephra horizons in the RESET lattice. Quat. Sci. Rev. 118, 18-32. https://doi.org/10.1016/j.quascirev.2014.11.007

Çağatay, M.N., Wulf, S., Sancar, Ü., Özmaral, A., Vidal, L., Henry, P., Appelt, O., Gasperini, L., 2015. The tephra record from the Sea of Marmara for the last ca. 70 ka and its palaeoceanographic implications. Mar. Geol. 361, 96-110. https://doi.org/10.1016/j.margeo.2015.01.005

Çağatay, M.N., Eriş, K.K., Makaroğlu, Ö., Yakupoğlu, N., Henry, P., Leroy, S.A.G., Uçarkuş, G., Sakınç, M., Yalamaz, B., Bozyiğit, C., Kende, J., 2019. The Sea of Marmara during Marine Isotope Stages 5 and 6. Quat. Sci. Rev. 220, 124-141. https://doi.org/10.1016/j.quascirev.2019.07.031

Di Paola, G.M., 1974.Volcanology and petrology of Nisyros Island (Dodecanese, Greece). B. Volcanol. 38, 944-987. https://doi.org/10.1007/BF02597100

Druitt, T.H., Edwards, L., Mellors, R.M., Pyle, D.M., Sparks, R.S.J., Lanphere, M., Davies, M., Barriero, B., 1999. Santorini Volcano. Geol. Soc. Spec. Publ. 19, 165 pp.

Fabbro, G.N., Druitt, T.H., Scaillet, S., 2013. Evolution of the crustal magma plumbing system during the build-up to the 22-ka caldera-forming eruption of Santorini (Greece). B. Volcanol. 75, 767. https://doi.org/10.1007/s00445-013-0767-5

Giaccio, B., Nomade, S., Wulf, S., Isaia, R., Sottili, G., Cavuoto, G., Galli, P., Messina, P., Sposato, A., Sulpizio, R., Zanchetta, G., 2012. The late MIS 5 Mediterranean tephra markers: a reappraisal from peninsular Italy terrestrial records. Quat. Sci. Rev. 56, 31-45. https://doi.org/10.1016/j.quascirev.2012.09.009

Giaccio, B., Hajdas, I., Isaia, R., Deino, A., Nomade, S., 2017. High-precision ^{14}C and $^{40}Ar/^{39}Ar$ dating of the Campanian Ignimbrite (Y-5) reconciles the time-scale of climatic cultural processes at 40 ka. Sci. Rep. 7, 45940. https://doi.org/10.1038/srep45940

Giaccio, B., Leicher, N., Mannella, G., Monaco, L., Regattieri, E., Wagner, B., Zanchetta, G., Gaeta, M., Marra, F., Nomade, S., Palladino, D.M., Pereira, A., Scheidt, S., Sottili, G., Wonik, T., Wulf, S., Zeeden, C., Aristegui, D., Cavinato, G.P., Dean, J.R., Florindo, F., Leng, M., Macrì, P., Niespolo, E., Renne, P.R., Rolf, C., Sadori, L., Thomas, C., Tzedakis, P.C., 2019. Extending the tephra and palaeoenvironmental record of the Central Mediterranean back to 430 ka: a new core from Fucino Basin, central Italy. Quat. Sci. Rev. 225, 106003. https://doi.org/10.1016/j.quascirev.2019.106003

Hardiman, J.C., 1999. Deep sea tephra from Nisyros Island, eastern Aegean Sea, Greece. Geol. Soc. Spec. Publ. 161, 69–88. https://doi.org/10.1144/GSL.SP.1999.161.01.06

Hunt, J.B., Hill, P.G., 1996. An inter-laboratory comparison of the electron probe microanalysis of glass geochemistry. Quatern. Int. 34-36, 229-241. https://doi.org/10.1016/1040-6182(95)00088-7

İşler, E.B., 2012. Paleoceanographic and paleoclimatic evolution of the Aegean Sea since the last Interglacial (~130 ka BP) with special emphasis on sapropel formation. PhD Thesis, Memorial University of Newfoundland. http://research.library.mun.ca/id/eprint/12114

İşler, E.B., Hiscott, R.N., Aksu, A.E., 2016. Late Quaternary chronostratigraphy of the Aegean Sea sediments: special reference to the ages of sapropels S1-S5. Turk. J. Earth Sci. 25, 1-18. https://doi.org/10.3906/yer-1501-37

Jochum, K.P., Stoll, B., Herwig, K., Willbold, M., Hofmann, A.W., et al., 2006. MPI-DING reference glasses for in situ microanalysis: New reference values for element concentrations and isotope ratios. Geochem. Geophy. Geosy. 7(2), Q02008. https://doi.org/10.1029/2005GC001060

Karkanas, P., White, D., Lane, C.S., Stringer, C., Davies, W., Cullen, V.L., Smith, V.C., Ntinou, M., Tsartsidou, G., Kyparissi-Apostolika, N., 2015. Tephra correlations and climatic events between the MIS6/5 transition and the beginning of MIS3 in Theopetra Cave, central Greece. Quat. Sci. Rev. 118, 170–181. https://doi.org/10.1016/j.quascirev.2014.05.027

Keller, J., Ryan, W.B.F., Ninkovich, D., Altherr, R., 1978. Explosive volcanic activity in the Mediterranean over the past 200,000 yr as recorded in deep-sea sediments. Geol. Soc. Am. Bull. 89, 591-604. https://doi.org/10.1130/0016-7606(1978)89%3C591:EVAITM%3E2.0.CO;2

Kuehn, S.C., Froese, D.G., Shane, P.A.R., INTAV Intercomparison Participants, 2011. The INTAV intercomparison of electron-beam microanalysis of glass by tephrochronology

laboratories: Results and recommendations. Quatern. Int. 246, 19-47. https://doi.org/10.1016/j.quaint.2011.08.022

Kwiecien, O., Arz, H.W., Lamy, F., Wulf, S., Bahr, A., Röhl, U., Haug, G.H., 2008. Estimated reservoir ages of the Black Sea since the last glacial. Radiocarbon 50(1), 99-118. https://doi.org/10.1017/S0033822200043393

Leicher, N., Zanchetta, G., Sulpizio, R., Giaccio, B., Wagner, B., Nomade, S., Francke, A., Del Carlo, P., 2016. First tephrostratigraphic results of the DEEP site record from Lake Ohrid (Macedonia and Albania). Biogeosciences 13, 2151-2178. https://doi.org/10.5194/bg-13-2151-2016

Limburg, E.M., Varekamp, J.C., 1991. Young pumice deposits on Nisyros, Greece. B. Volcanol. 54(1), 68–77. https://doi.org/10.1007/BF00278207

Longchamp, C., Bonadonna, C., Bachmann, O., Skopelitis, A., 2011. Characterization of tephra deposits with limited exposure: the example of the two largest explosive eruptions at Nisyros volcano (Greece). B. Volcanol. 73, 1337-1352. https://doi.org/10.1007/s00445-011-0469-9

Lowe, D.J., 2011. Tephrochronology and its application: A review. Quat. Geochronol. 6, 107-153. https://doi.org/10.1016/j.quageo.2010.08.003

Margari, V., Pyle, D.M., Bryant, C., Gibbard, P.L., 2007. Mediterranean tephra stratigraphy revisited: Results from a long terrestrial sequence on Lesvos Island, Greece. J. Volcanol. Geoth. Res. 163, 34-54. https://doi.org/10.1016/j.jvolgeores.2007.02.002

Margari, V., Gibbard, P.L., Bryant, C.L., Tzedakis, P.C., 2009. Character of vegetational and environmental changes in southern Europe during the last glacial period; evidence from Lesvos Island, Greece. Quat. Sci. Rev. 28, 1317-1339. https://doi.org/10.1016/j.quascirev.2009.01.008

Martin-Puertas, C., Brauer, A., Wulf, S., Ott, F., Lauterbach, S., Dulski, P., 2014. Annual proxy data from Lago Grande di Monticchio (southern Italy) between 76 and 112 ka: new chronological constraints and insights on abrupt climatic oscillations. Clim. Past 10, 2099-2114. https://doi.org/10.5194/cp-10-2099-2014

Milner, A.M., Roucoux, K.H., Collier, R.E.L., Müller, U.C., Pross, J., Tzedakis, P.C., 2016. Vegetation responses to abrupt climatic changes during the Last Interglacial Complex (Marine Isotope Stage 5) at Tenaghi Philippon, NE Greece. Quat. Sci. Rev. 154, 169-181. https://doi.org/10.1016/j.quascirev.2016.10.016

Müller, U.C., Pross, J., Tzedakis, P.C., Gamble, C., Kotthoff, U., Schmiedl, G., Wulf, S., Christanis, K., 2011. The role of climate in the spread of modern humans into Europe. Quat. Sci. Rev. 30, 273-279. https://doi.org/10.1016/j.quascirev.2010.11.016

444 Narcisi, B., Vezzoli, L., 1999. Quaternary stratigraphy of distal tephra layers in the
445 Mediterranean - an overview. Global Planet. Change 21, 31-50.
446 https://doi.org/10.1016/S0921-8181(99)00006-5
447 NGRIP members, 2004. High-resolution record of Northern Hemisphere climate extending
448 into the last interglacial period. Nature 431, 147-151. https://doi.org/10.1038/nature02805
449 Pe-Piper, G., Moulton, B., 2008. Magma evolution in the Pliocene-Pleistocene succession of
450 Kos, South Aegean arc (Greece). Lithos 106(1–2), 110–124.
451 https://doi.org/10.1016/j.lithos.2008.07.002
452 Popa, R.-G., Guillong, M., Bachmann, O., Szymanowski, D., Ellis, B., 2020. U-Th zircon
453 dating reveals a correlation between eruptive styles and repose periods at the Nisyros-
454 Yali volcanic area, Greece. Chem. Geol. 555, 11930.
455 https://doi.org/10.1016/j.chemgeo.2020.119830
456 Pyle, D.M., Margari, V., 2009. Reply: Correlation of a widespread Pleistocene tephra marker
457 from the Nisyros-Yali volcanic complex, Greece. J. Volcanol. Geoth. Res. 181, 251-254.
458 https://doi.org/10.1016/j.jvolgeores.2008.11.033
459 Rehren, T., 1988. Geochemie und Petrologie von Nisyros (Ostliche Agais). PhD thesis,
460 University of Freiburg, pp. 167.
461 Reimer, P.J., Austin, W.E.N., Bard, E., Bayliss, A., Blackwell, P.G., Bronk Ramsey, C.,
462 Butzin, M., Cheng, H., Edwards, R.L., Friedrich, M., Grootes, P.M., Guilderson, T.P.,
463 Hajdas, I., Heaton, T.J., Hogg, A.G., Hughen, K.A., Kromer, B., Manning, S.W.,
464 Muscheler, R., Palmer, J.G., Pearson, C., van der Plicht, J., Reimer, R.W., Richards,
465 D.A., Scott, E.M., Southon, J.R., Turney, C.S. M., Wacker, L., Adolphi, F., Büntgen, U.,
466 Capano, M., Fahrni, S.M., Fogtmann-Schulz, A., Friedrich, R., Köhler, P., Kudsk, S.,
467 Miyake, F., Olsen, J., Reinig, F., Sakamoto, M., Sookdeo, A., Talamo, S., 2020. The
468 IntCal20 Northern Hemisphere Radiocarbon Age Calibration Curve (0–55 cal kBP).
469 Radiocarbon 62(4), 725–757. https://doi.org/10.1017/RDC.2020.41
470 Sánchez Goñi, M.F., Desprat, S., Daniau, A.-L., Bassinot, F.C., Polanco-Martínez, J.M.,
471 Harrison, S.P., Allen, J.R.M., Anderson, R.S., Behling, H., Bonnefille, R., Burjachs, F.,
472 Carrión, J.S., Cheddadi, R., Clark, J.S., Combourieu-Nebout, N., Courtney-Mustaphi,
473 C.J., Debusk, G.H., Dupont, L.M., Finch, J.M., Fletcher,W.J., Giardini, M., González, C.,
474 Gosling, W.D., Grigg, L.D., Grimm, E.C., Hayashi, R., Helmens, K., Heusser, L.E., Hill, T.,
475 Hope, G., Huntley, B., Igarashi, Y., Irino, T., Jacobs, B., Jiménez-Moreno, G., Kawai, S.,
476 Kershaw, P., Kumon, F., Lawson, I.T., Ledru, M.-P., Lezine, A.-M., Liew, P.M., Magri, D.,
477 Marchant, R., Margari, V., Mayle, F.E., McKenzie, M., Moss, P., Müller, S., Müller, U.C.,
478 Naughton, F., Newnham, R.M., Oba, T., Pérez-Obiol, R., Pini, R., Ravazzi, C., Roucoux,
479 K.H., Rucina, S.M., Scott, L., Takahara, H., Tzedakis, P.C., Urrego, D.H., van Geel, B.,
480 Valencia, B.G., Vandergoes, M.J., Vincens, A., Whitlock, C.L., Willard, D.A., Yamamoto,

M., 2017. The ACER pollen and charcoal database: a global resource to document vegetation and fire response to abrupt climate changes during the last glacial period. Earth Syst. Sci. Data 9 (2), 679-695. https://doi.org/10.5194/essd-2017-4.

Satow, C., Tomlinson, E.L., Grant, K.M., Albert, P.G., Smith, V.C., Manning, C.J., Ottolini, L., Wulf, S., Rohling, E.J., Lowe, J.J., Blockley, S.P.E., Menzies, M.A., 2015. A new contribution to the Late Quaternary tephrostratigraphy of the Mediterranean: Aegean Sea core LC21. Quat. Sci. Rev. 117, 96-112. https://doi.org/10.1016/j.quascirev.2015.04.005

Satow, C., Grant, K., Wulf, S., Schulz, H., Mallon, A., Matthews, I, Lowe, J., 2020. Detection and characterisation of Eemian marine tephra layers within the sapropel S5 sediments of the Aegean and Levantine Seas. Quaternary 3(1), 6. https://doi.org/10.3390/quat3010006

Scaillet, S., Vita-Scaillet, G., Rotolo, S.G., 2013. Millennial-scale phase relationships between ice-core and Mediterranean marine records: insights from high-precision $^{40}Ar/^{39}Ar$ dating of the Green Tuff of Pantelleria, Sicily Strait. Quat. Sci. Rev. 78, 141-154. https://doi.org/10.1016/j.quascirev.2013.08.008

Smith, P.E., York, D., Chen, Y., Evensen, N.M., 1996. Single crystal ^{40}Ar-^{39}Ar dating of a Late Quaternary paroxysm on Kos, Greece: Concordance of terrestrial and marine ages. Geophys. Res. Lett. 23, 3047-3050. https://doi.org/10.1029/96GL02759

Svensson, A., Andersen, K.K., Bigler, M., Clausen, H.B., Dahl-Jensen, D., Davies, S.M., Johnsen, S.J., Muscheler, R., Rasmussen, S.O., Röthlisberger, R., Steffensen, J.P., Vinther, B.M., 2006. The Greenland Ice Core Chronology 2005, 15-42 ka. Part 2: comparison to other records. Quat. Sci. Rev. 25, 3258-3267. https://doi.org/10.1016/j.quascirev.2006.08.003

Svensson, A., Andersen, K.K., Bigler, M., Clausen, H.B., Dahl-Jensen, D., Davies, S.M., Johnsen, S.J., Muscheler, R., Parrenin, F., Rasmussen, S.O., Röthlisberger, R., Seierstad, I., Steffensen, J.P., Vinther, B.M., 2008. A 60000-year Greenland stratigraphic ice core chronology. Clim. Past 4, 47-57. https://doi.org/10.5194/cp-4-47-2008

Tomlinson, E.L., Kinvig, H.S., Smith, V.C., Blundy, J.D., Gottsmann, J., Müller, W., Menzies, M.A., 2012a. The Upper and Lower Nisyros Pumices: revisions to the Mediterranean tephrostratigraphic record based on micron-beam glass geochemistry. J. Volcanol. Geoth. Res. 243-244, 69–80. https://doi.org/10.1016/j.jvolgeores.2012.07.004

Tomlinson, E.L., Arienzo, I., Civetta, L., Wulf, S., Smith, V.C., Hardiman, M., Lane, C.S., Carandente, A., Orsi, G., Rosi, M., Muller, W., Menzies, M.A., 2012b. Geochemistry of the Phlegraean Fields (Italy) proximal sources for major Mediterranean tephras: Implications for the dispersal of Plinian and co-ignimbritic components of explosive eruptions. Geochim. Cosmochim. Ac. 93, 102-128. https://doi.org/10.1016/j.gca.2012.05.043

Tomlinson, E.L., Smith, V.C., Albert, P.G., Aydar, E., Civetta, L., Cioni, R., Çubukçu, E., Gertisser, R., Isaia, R., Menzies, M.A., Orsi, G., Rosi, M., Zanchetta, G., 2015. The major

and trace element glass compositions of the productive Mediterranean volcanic sources: tools for correlating distal tephra layers in and around Europe. Quat. Sci. Rev. 118, 48-66. https://doi.org/10.1016/j.quascirev.2014.10.028

Vakhrameeva, P., Koutsodendris, A., Wulf, S., Fletcher, W.J., Appelt, O., Knipping, M., Gertisser, R., Trieloff, M., Pross, J., 2018. The cryptotephra record of the Marine Isotope Stage 12 to 10 interval (460-335 ka) at Tenaghi Philippon, Greece: Exploring chronological markers for the Middle Pleistocene of the Mediterranean region. Quat. Sci. Rev. 200, 313–333. https://doi.org/10.1016/j.quascirev.2018.09.019

Vakhrameeva, P., Wulf, S., Koutsodendris, A., Tjallingii, R., Fletcher, W.J., Appelt, O., Ludwig, T., Knipping, M., Trieloff, M., Pross, J., 2019. Eastern Mediterranean volcanism during Marine Isotope Stages 9 to 7e (335–235 ka): Insights based on cryptotephra layers at Tenaghi Philippon, Greece. J. Volcanol. Geoth. Res. 380, 31–47. https://doi.org/10.1016/j.jvolgeores.2019.05.016

Vinci, A., 1983. A new ash layer 'Nisyros Layer' in the Aegean Sea sediments. Bollettino di Oceanologia Teorica ed Applicata 1, 341–342.

Vinci, A., 1985. Distribution and chemical composition of tephra layers from Eastern Mediterranean abyssal sediments. Mar. Geol. 64, 143-155. https://doi.org/10.1016/0025-3227(85)90165-3

Vogel, H., Wagner, B., Zanchetta, G., Sulpizio, R., Rosén, P., 2010. A Paleoclimate record with tephrochronological age control for the last glacial-interglacial cycle from lake Ohrid, Albania and Macedonia. J. Paleolimnol. 44, 295-310. https://doi.org/10.1007/s10933-009-9404-x

Wegwerth, A., Dellwig, O., Wulf, S., Plessen, B., Kleinhanns, I.C., Nowaczyk, N.C., Jiabo, L., Arz, H.W., 2019. Major hydrological shifts in the Black Sea "Lake" in response to ice sheet collapses during MIS 6 (130-184 ka BP). Quat. Sci. Rev. 219, 126-144. https://doi.org/10.1016/j.quascirev.2019.07.008

Wolff, E.W., Chappellaz, J., Blunier, T., Rasmussen, S.O., Svensson, A., 2010. Millennial-scale variability during the last glacial: The ice core record. Quat. Sci. Rev. 29, 2828-2838. https://doi.org/10.1016/j.quascirev.2009.10.013

Wulf, S., Keller, J., Paterne, M., Mingram, J., Lauterbach, S., Opitz, S., Sottili, G., Giaccio, B., Albert, P.G., Satow, C., Tomlinson, E.L., Viccaro, M., Brauer, A., 2012. The 100-133 ka record of Italian explosive volcanism and revised tephrochronology of Lago Grande di Monticchio. Quat. Sci. Rev. 58, 104–123. https://doi.org/10.1016/j.quascirev.2012.10.020

Wulf, S., Hardiman, M., Staff, R.A., Koutsodendris, A., Appelt, O., Blockley, S.P.E., Lowe, J.J., Manning, C.J., Ottolini, L., Schmitt, A.K., Smith, V.C., Tomlinson, E.L., Vakhrameeva, P., Knipping, M., Kotthoff, U., Milner, A.M., Müller, U.C., Christanis, K., Kalaitzidis, S., Tzedakis, C., Schmiedl, G., Pross, J., 2018. The Marine Isotope Stage

1 to 5 cryptotephra record of Tenaghi Philippon, Greece: Towards a detailed tephrostratigraphic framework for the Eastern Mediterranean region. Quat. Sci. Rev. 186, 236-262. https://doi.org/10.1016/j.quascirev.2018.03.011

Wulf, S., Keller, J., Satow, C., Gertisser, R., Kraml, M., Grant, K.M., Appelt, O., Vakhrameeva, P., Koutsodendris, A., Hardiman, M., Schulz, H., Pross, J., 2020. Advancing Santorini's tephrostratigraphy: new glass geochemical data and improved marine-terrestrial tephra correlations for the past ~360 kyrs. Earth-Sci. Rev. 200, 102964. https://doi.org/10.1016/j.earscirev.2019.102964

Supplement A: *EPMA glass data of tephra layers MT-1, MT-2 and MT-3 from cores MRS-CS18 and MRS-CS27; EPMA glass reference data for data control; Bayesian age models of cores MRS-CS18 and MRS-CS27.*

Supplement Table B1: *Revised age constraints (radiocarbon, tephra) of Sea of Marmara sediment cores MRS-CS18 and MRS-CS27.*

Supplement Figure B1: *OxCal age-depth models of cores MRS-CS18 and MRS-CS27.*

Supplement Figure B2: *Comparison of original and revised age-depth models of Megali Limni core ML01.*

Supplement Figure B3*: Selected pollen taxa (Total tree taxa, Juniper+Pinus, and Artemisia) of the ML01 sequence from Megali Limni on a depth scale.*

Supplement Figure B4: *Selected pollen taxa (Total tree taxa, Juniper+Pinus, and Artemisia) of the ML01 sequence from Megali Limni on a revised time scale (this study).*

Supplement C: *Revised age constraints and Bayesian age model of Megali Limni core ML01 (this study); ML01 pollen dataset from Margari et al. (2009) and Sánchez Goñi et al. (2017) on a revised timescale; Age constraints used for the original ML01 chronology of Margari et al. (2007, 2009).*